Journal of Materials Chemistry B

Accepted Manuscript

ROYAL SOCIETY OF CHEMISTRY

www.rsc.org/materialsB

Journal Name

ARTICLE

Boron ketoiminate-based conjugated polymers with tunable AIE behaviours and their applications for cell imaging†

Received 00th January 20xx,
Accepted 00th January 20xx

DOI: 10.1039/x0xx00000x

www.rsc.org/

Chunhui Dai,[a] Dongliang Yang,[b] Wenjie Zhang,[a] Xiao Fu,[b] Qingmin Chen,[a] Chengjian Zhu,[a] Yixiang Cheng*[a] and Lianhui Wang*[b]

Three new boron ketoiminate-based conjugated polymers **P1**, **P2**, and **P3** were designed and synthesized through Sonogashira coupling reaction of 4,6-bis(4-bromophenyl)-2,2-difluoro-3-phenyl-2*H*-1,3,2-oxazaborinin-3-ium-2-uide (**M1**) with 1,4-diethynyl-2,5-bis(octyloxy)benzene (**M2**), 3,6-diethynyl-9-octyl-9*H*-carbazole (**M3**) and 3,7-diethynyl-10-octyl-10*H*-phenothiazine-*S*,*S*-dioxide (**M4**), respectively. All the resulting polymers showed obvious aggregation-induced emission (AIE) behaviours. Interestingly, it was found that great difference on the electron-donating abilities of the D-A type polymer linkers can lead to the unique AIE behaviours of the alternating polymers in the aggregate state, which provides us with a practical strategy to design tunable AIE-active conjugated polymers. Most importantly, studies on MCF-7 breast cancer cell imaging revealed that the nanoparticles fabricated from the conjugated polymers could serve as promising fluorescent probes with low cytotoxity and high photosability.

Introduction

In the past few years, donor–acceptor (D–A) type conjugated polymers (CPs) have received much attention due to their various optoelectronic applications for solar cells,[1] thin film transistors (TFTs),[2] field-effect transistors (FETs),[3] electrochromic devices,[4] and memory devices,[5] *etc*. As one of the most promising strategies to improve optical properties of CPs in the organic electronics research field, development on the D-A approach is mainly focused on the conjugated polymer with a delocalized π-electron system that comprises alternating electron-rich (donor) and electron-deficient (acceptor) repeating units. The energy level of the polymer can be finely tuned though intramolecular charge transfer (ICT) based on the dipole-dipole interactions between alternating donors and acceptors.[6] Previously, our studies on D-π-A type CPs demonstrated that the incorporation of near-infrared (NIR) emissive chromophores into π-conjugated polymer backbones could give narrow band emissive polymers (even lower than 1.25 eV), which are potential materials for device-based applications.[7] However, most of D-A type compounds encounter notorious aggregation-caused quenching (ACQ) effect in the aggregate state, which causes a significant decrease in the fluorescence intensity in aqueous system and thus limits their applications for bioimaging.[8] To overcome this limitation, it is highly desirable to develop novel D-A CPs with strong fluorescence emission in the aqueous solution. Currently, aggregation-induced emission (AIE)-active polymer materials have attracted great interest. The luminogenic materials with AIE characteristics are non-emissive or weakly fluorescent when dissolved in the dilute solutions, but the fluorescence intensity greatly increase in their aggregations.[9] Because of highly emissive efficiency when aggregated in water, AIEgens have been used as powerful materials for biomedical applications.[10]

Recently, more and more works demonstrated that the fluorophores with D−A systems can show AIE characteristics in highly polar aqueous media, the AIE-ICT luminogens can exhibit high solid emission efficiency and potential biological and optoelectronic device applications.[11] Our group recently also found that the AIE properties of dicyanomethylene-1,4-dihydropyridine derivatives can be effectively tuned by intramolecular D-π-A conjugated structure systems.[12] In the present work, we designed and synthesized a series of boron ketoiminate-based alternating D-π-A type CPs for live cell imaging (Scheme 1). Herein, boron ketoiminate was chosen as an AIE-active unit with excellent optical properties.[13] Importantly, it can also act as an acceptor in the conjugated polymer backbone. To the best of our knowledge, there has been few researches on D-π-A type boron ketoiminate-based conjugated polymers with tunable AIE activities. Furthermore, the polymers were used to prepare conjugated polymer nanoparticles (CPNs) by a simple reprecipitaion method. The obtained CPNs suspension showed high photostability and low cytotoxicity and were successfully employed for MCF-7 cancer cell imaging.

[a] *Key Lab of Mesoscopic Chemistry of MOE, School of Chemistry and Chemical Engineering, Nanjing University, Nanjing 210093, China. E-mail: yxcheng@nju.edu.cn. Tel: +86-25-83686508*
[b] *Key Laboratory for Organic Electronics and Information Displays and Institute of Advanced Materials, Nanjing University of Posts and Telecommunications, Nanjing, 210023, China. E-mail: iamlhwang@njupt.edu.cn*
† Electronic Supplementary Information (ESI) available. See
DOI: 10.1039/x0xx00000x

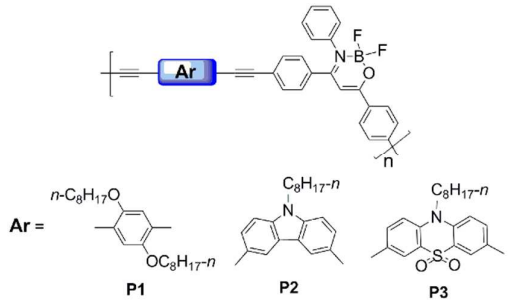

Scheme 1 Chemical structures of the conjugated polymers.

Results and discussion

Synthesis and characterization

The detailed synthetic procedures of the monomers and conjugated polymers are illustrated in Scheme S1 (ESI 2). To synthesize the targeted conjugated polymers, we first synthesized the corresponding monomer units. The monomer **M1** was obtained by the condensation reaction of aniline (**1**) with (*Z*)-1,3-bis(4-bromophenyl)-3-hydroxyprop-2-en-1-one (**2**) in the presence of a catalytic amount of *p*-toluenesulfonic acid, followed by coordination with trifluorobonetherate in the presence of triethylamine. The monomers **M2-M4** were synthesized by our previously reported procedure (ESI 2). The polymerization was accomplished by the Pd(II)-catalyzed Sonogashira coupling reaction of **M1** with **M2**, **M3**, and **M4** in the presence of a catalytic amount of $[Pd(PPh_3)_4]$ and CuI, to afford **P1**, **P2**, and **P3**, respectively. In a typical experiment, the polymerizations were carried out in a degassed mixture of anhydrous THF and anhydrous Et_3N under N_2 at 80 °C for 24 h. The polymers were precipitated from methanol, filtered, and dried in vacuum. The number average molecular weight (M_n) was determined to be 8210 g mol^{-1} (PDI = 2.49) for **P1**, 4220 g mol^{-1} (PDI = 2.62) for **P2**, and 4750 g mol^{-1} (PDI = 2.18) for **P3** by GPC using a polystyrene standard in THF. All the obtained conjugated polymers showed good solubility in common organic solvents, such as THF, toluene, CH_2Cl_2, $CHCl_3$, which can be attributed to the flexible *n*-octyl substituents.

Optical properties

The photophysical properties of **P1-P3** in THF solutions and aggregated states (10 μM) were measured using UV-vis absorption and photoluminescence (PL) spectra, and the relevant data are summarized in Table 1. As shown in Figure 1, **P1**, **P2**, and **P3** in THF solutions all exhibited a strong absorption peak at 234 nm, which could be ascribed to strong $S_0 \rightarrow S_2$ (π–π^*) transition. In addition, **P1**, **P2**, and **P3** showed a weak shoulder peak at 318 nm, 296 nm and 292 nm, respectively. Another broad peak emerged at 418 nm for **P1**, 410 nm for **P2**, and 386 nm for **P3**, respectively, which could be regarded as $S_0 \rightarrow S_1$ (π–π^*) transition. The longer absorption bands of the three polymers are attributed to an intramolecular charge transfer (ICT) band between donors and acceptors.

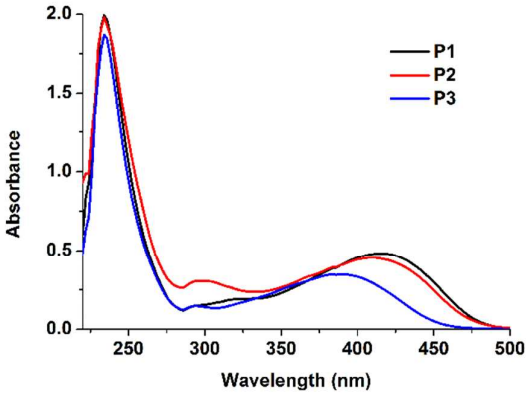

Fig. 1 UV/vis absorption spectra of **P1-P3** in THF solution (10 μM).

The AIE behaviours of **P1-P3** were investigated in THF/water mixtures at different water fractions (f_w). As shown in Figure 2a, **P1** was almost non-emissive in THF solution and the intensities had very small changes when f_w varied from 0 to 60%. When f_w was 70% or higher, the intensity enhanced significantly and reached nearly 27-fold greater than that in pure THF solution (Figure 2d). **P2** in THF dilute solution also showed faint PL signals peaking at 553 nm. When more water was added, the emission enhanced with red-shifted maximum emission wavelength of 563 nm, which can be related to aggregate formation. The emission intensity in 80% aqueous mixture reached more than 9-fold higher than that of pure THF solution, which was the AIE characteristic. However, when f_w came to 90%, the emission was badly quenched. The decreased emission intensity can be ascribed to twisted intramolecular charge transfer (TICT) resulting from the gradually increasing polarity of the solvent mixture, which is often seen in AIE-active molecules with D-A structures.[14,15] **P3** showed similar AIE behaviors with **P2**. **P3** exhibited a very weak emission in THF solution with an emission peak at 460 nm. The emission increased slowly as f_w progressively increased from 0 to 50%. Meanwhile, the emission maximum was red-shifted to around 550 nm. When f_w = 90%, the fluorescence intensity reached the maximum (18-fold comparing with it in pure solution) and the peak was blue-shifted to 545 nm. With the increase of the water fraction, the aggregates of **P3** may possess a conformation twisting of the conjugated backbone, which leads to a decrease of the effective conjugation length, thus results in unusual blue-shifted emission.[15e] When f_w = 100%, the intensity decreased in a small range. Finally, when f_w =100%, the enhancement of PL intensity were only 6-fold for **P2** (Figure 2e), and 17-fold for **P3** (Figure 2f), respectivley. These results implied that the D-A interactions in **P1-P3** exerted influence on the emission wavelength and efficiency of the luminogens in aggregated states.

Table 1. Summary data of optical properties of **P1-P3**.

	In THF (1×10^{-5} mol/L) [a]			CPNs [a]	
polymer	λ_{abs} (nm)	λ_{PL} (nm)	Φ [b]	λ_{PL}(nm)	Φ [b]
P1	234, 318, 418	459	<0.01	551	0.14
P2	234, 296, 410	553	<0.01	563	0.06
P3	234, 292, 386	460	<0.01	545	0.11

[a] Excited at 405 nm. [b] Quantum yields were determined with Coumarine 153 in ethanol (Φ = 0.38) as the fluorescence reference.

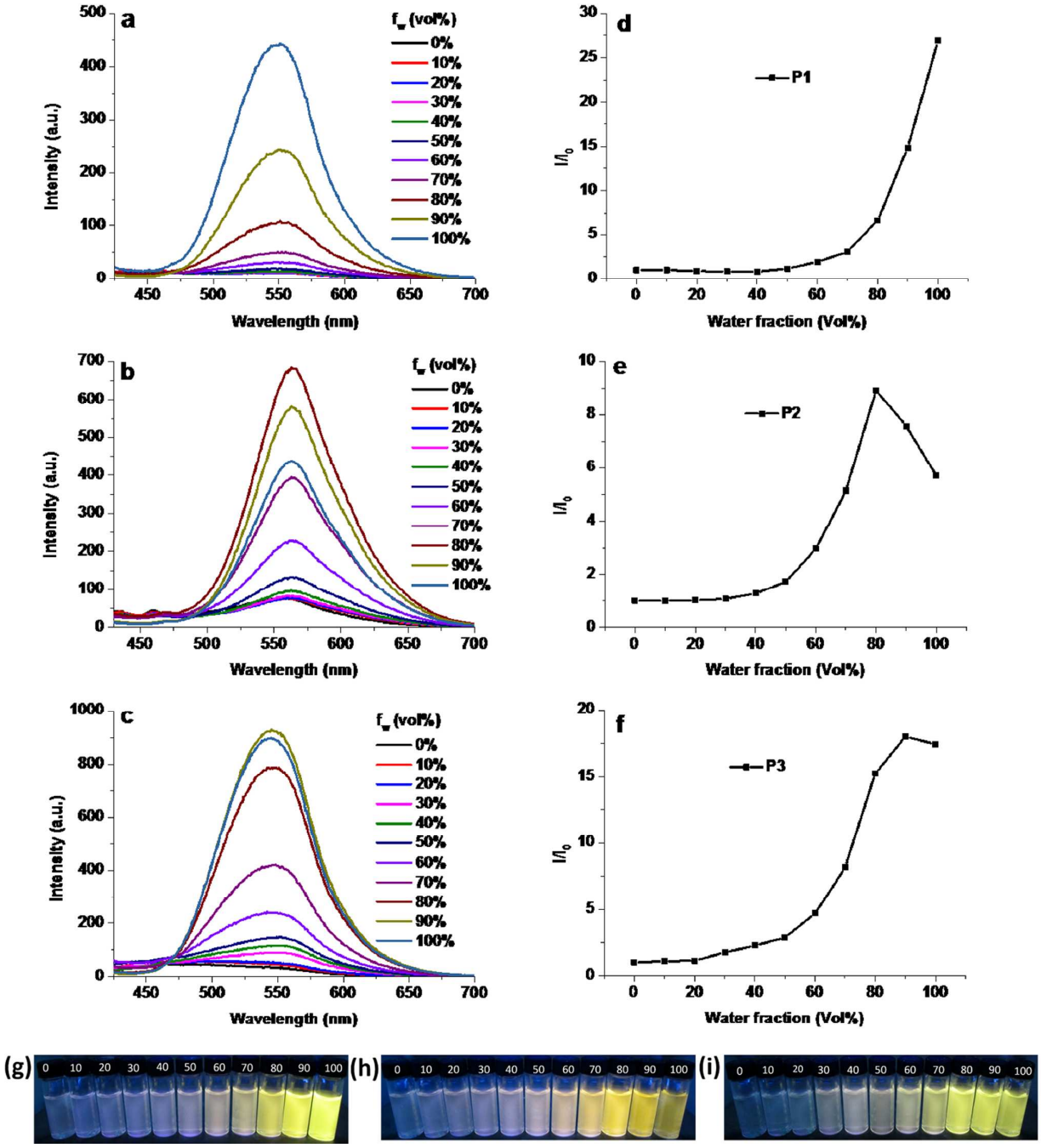

Fig. 2 Fluorescence spectra of (a) **P1**, (b) **P2**, and (c) **P3** in THF/water mixtures with different water fractions and plot of I/I_0 of (d) **P1**, (e) **P2**, and (f) **P3** versus the volume fraction of water in THF/water mixtures, where where I_0 and I are the emission intensity in pure THF solution and THF/water mixture, respectively. Photographs of solutions of (g) **P1**, (h) **P2**, (i) **P3** in THF/ water mixtures with different water fractions taken under UV illumination. The concentration of all solutions and suspensions is 10 μM, excited at 405 nm.

Preparation and characterization of CPNs

P1-P3 NPs were prepared by using the reprecipitation method as described previously.[16] In brief, the conjugated polymer in dilute THF solution was injected rapidly into Milli-Q water under ultrasonication. CPNs suspension was obtained after vacuum removal of the THF. The particle size and morphology of the CPNs were characterized by transmission electron microscopy (TEM) and dynamic light scattering (DLS) (Figure S4 in ESI 9). The TEM images illustrate that the CPNs exhibit

spherical shape with particle diameters of ~63 nm, ~55 nm, and ~57 nm for **P1**, **P2** and **P3**, respectively. As indicated by DLS, the average diameters of the CPNs are 79.5 nm, 69.5 nm, and 71.7 nm for **P1**, **P2** and **P3**, respectively. The CPNs disperse homogeneously in the water without aggregates. The fluorescence quantum yields were determined to be 0.14, 0.06, and 0.11 for the NPs suspension of **P1**, **P2**, and **P3**, respectively. In addition, to better understand emission dynamics of CPNs and the fluorescence decay process, the fluorescence lifetimes of the CPNs suspensions were measured by time resolved technique. The fluorescence emission lifetime of CPNs are determined to be 2.09 ns for **P1** NPs, 5.20 ns for **P2** NPs, and 2.04 ns for **P3** NPs, respectively, with the mean square deviation χ^2 (CHISQ) values ranging from 1.053 and 1.145 (Figure S5 and S6 in ESI 10).

Electrochemical properties

To determine the frontier orbital levels, the electrochemical properties of all the conjugated polymers were evaluated using cyclic voltammetry. The cyclic voltammograms were recorded in anhydrous CH_2Cl_2 solution with 0.1 M tetrabutylammonium hexauorophosphate (Bu_4NPF_6) as the supporting electrolyte at a scan rate of 50 mV/s. A platinum wire was used as the counter electrode and an Ag/AgCl reference electrode, and redox potentials were calibrated using the ferrocene/ferrocenium (Fc/Fc^+) redox couple. The CV curves of **P1-P3** are shown in Figure 3, and the onset oxidation and reduction potentials along with the estimated HOMO and LUMO energy levels are summarized in Table 2. As a result, the HOMO/LUMO energy

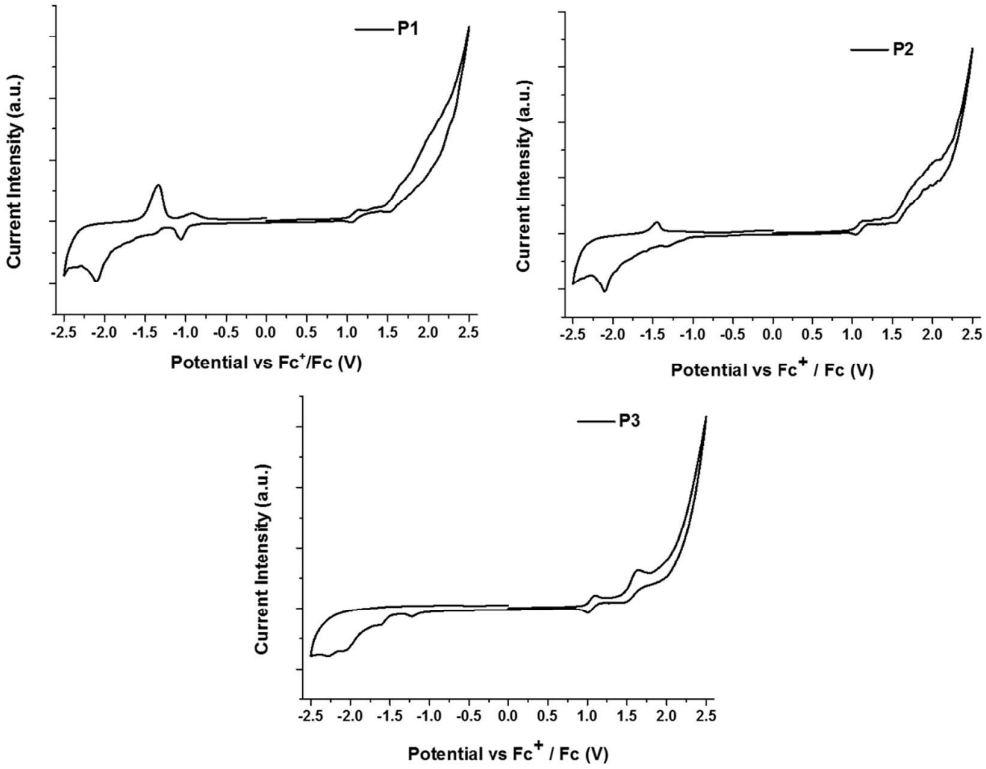

Fig. 3 Cyclic voltammograms of **P1**-**P3** in deoxygenated CH_2Cl_2 solution containing Bu_4NPF_6 (0.1 M)

Table 2 Electrochemical properties and calculated HOMO and LUMO energy levels of **P1-P3**

polymer	From CV [a]					From calculation		
	$E_{ox,onset}$ [b] [V]	HOMO [eV]	$E_{red,onset}$ [b] [V]	LUMO [eV]	E_g [c] [eV]	HOMO [eV]	LUMO [eV]	E_g [d] [eV]
P1	1.02	-5.82	-0.94	-3.86	1.96	-5.76	-2.49	3.27
P2	0.97	-5.77	-0.97	-3.83	1.94	-5.37	-2.31	3.06
P3	0.98	-5.78	-1.02	-3.78	2.00	-5.72	-2.47	3.25

[a] The ferrocence couple (Fc/Fc^+) was used as the internal reference and under our experimental conditions, $E(Fc^+/Fc)$ = 0.42 V *vs.* Ag/AgCl. [b] E_{ox} and E_{red} determined from the onset potentials of the oxidation and reduction waves, respectively. [c] Optical band gap (E_g), E_g = LUMO - HOMO. [d] DFT quantum mechanical calculations (B3LYP/6–31 G*). HOMO = – (E_{ox} + 4.8) eV and LUMO = – (E_{red} + 4.8) eV.

levels of the polymers, estimated from the oxidation/reduction onset, were -5.82/-3.86 eV for **P1**, -5.77/-3.83 eV for **P2**, and -5.78/-3.78 eV for **P3**, and thus corresponding electrochemical bandgaps of **P1**, **P2**, and **P3** were determined to be 1.96, 1.94, and 2.00 eV, respectively.[17]

Molecular orbital calculations

To assess the influence of donor on the frontier optical energies, DFT calculations were performed on the three optimized model molecules constituting the corresponding repeating units shown in Figure 4 at the B3LYP/6-31g (2d, p) level with the Gaussian 09 A.02 package.[18] In the calculations, the long alkyl chains on the polymer backbones were replaced with methyl groups. The calculated LUMO/HOMO energy level of model 1-3 are -2.49/-5.76, -2.31/-5.37, -2.47/-5.72, respectively. The LUMO of the model compounds is mainly centred on the boron-ketoiminate unit because it is an acceptor. Compared to model 1 and 3, model 2 shows a highest HOMO level, suggesting carbazole unit has a higher electron-donating ability compared to benzene and phenothiazine-*S*,*S*-dioxide units. Because of the strong D-A interaction between boron ketoiminate unit and the carzole group, the HOMO-LUMO band gap of model 2 (3.06 eV) is smaller than those of model 1 (3.27 eV) and model 3 (3.25 eV), which is consistent with the electrochemical results discussed above.

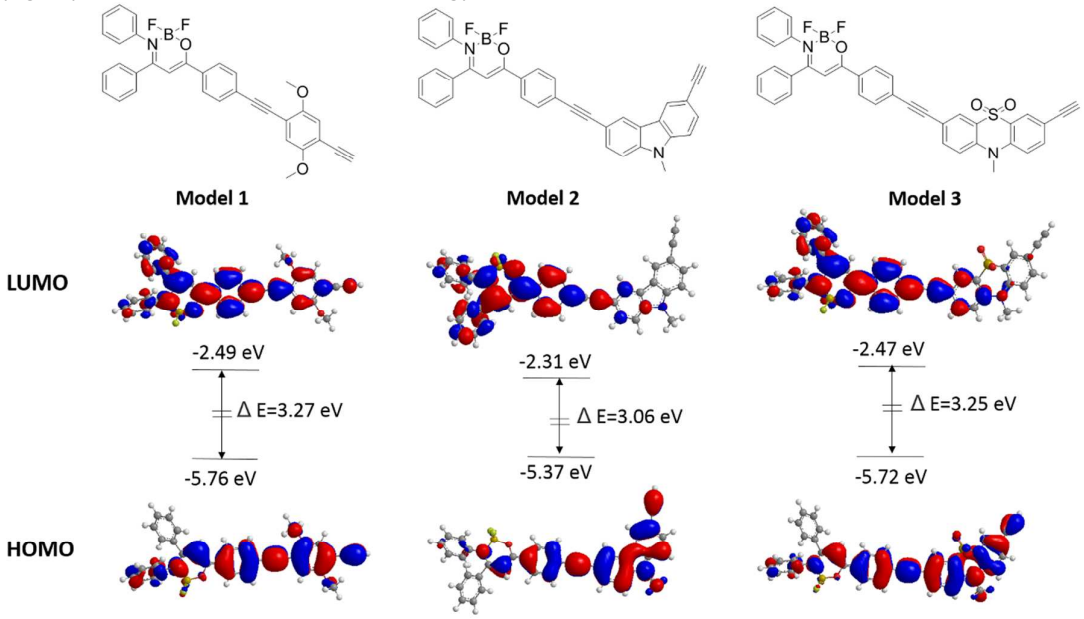

Fig. 4 Optimized model compounds from **P1-P3** for DFT calculations and Molecular orbital diagrams for the LUMO and HOMO of Model 1-3.

Cytotoxicity and photostability

To evaluate the cytotoxicity of the **P1-P3** NPs, the metabolic viability of MCF-7 cells after incubation with CPNs was investigated at different nanoparticle suspension concentrations. Figure 5a-c shows the cytotoxicity results of the **P1-P3** NPs upon incubation with suspension at 0 to 40 μM for 48 h, respectively. The cell viabilities remain above 90% upon incubation with NPs for 48 h at the concentration of 40 μM, indicating the low cytotoxicity of the probes, which is ideal for bioimaging. Excellent photostability in water is crucial for bioimaging because high photostability can effectively resist photobleaching and allows the imaging process to last for a long period. We evaluated the photostability of **P1-P3** NPs by using CLSM and analysed the intensity changes upon incubation with PBS buffer solution at 37 °C for 0-10 minutes. As shown in Figure 5d, upon continuous excitation at 405 nm (5 mW) for 10 min, PL intensity loss of **P1**, **P2**, **P3** NPs are only 10%, 14%, 12%, respectively. The observation indicates all the CPNs have good photostability and are promising in bioimaging.

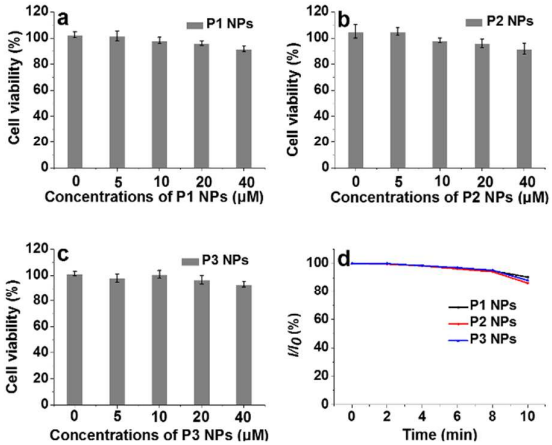

Fig. 5 (a-c) Metabolic viability of MCF-7 cells after incubation with **P1-P3** NPs suspension at different concentrations for 48 h. (d) Photostability of **P1-P3** NPs upon continuous laser excitation at 405 nm with a laser power of 5 mW for 0-10 min. I_0 is the initial fluorescence intensity and I is the fluorescence intensity of each sample at different time intervals after continuous laser scanning.

Cell imaging application of CPNs

Inspired by the excellent photophysical performance of **P1-P3** NPs suspension, we subsequently applied them in cell imaging. The in vitro cellular imaging was accessed by CLSM using MCF-7 cancer cells as the example cell line and fluorescence imaging were conducted upon excitation at 405 nm. The fluorescence images of MCF-7 cancer cell were obtained after treatment with ~4 μM of **P1-P3** NPs suspension for 2 h at 37 °C, respectively. As is evident from Figure 6a-c, it can be clearly observed that the CPNs mainly locate in the cell cytoplasm around the nuclei of MCF-7 cells, which demonstrates that the CPNs could be effectively taken up by MCF-7 cells. Meanwhile, a little aggregation could be observed on the cell membrane, which is attributed to the large particle size of CPNs.

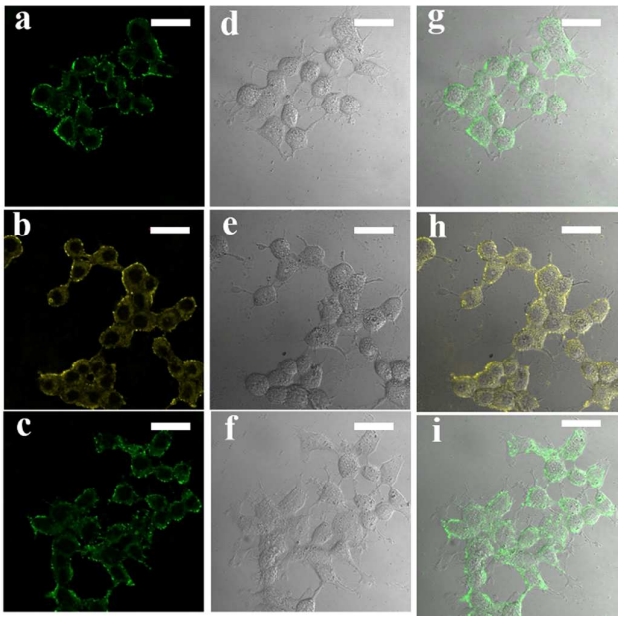

Fig. 6 Confocal laser scanning microscopy (CLSM) images of the MCF-7 cells stained with (a) **P1**, (b) **P2**, and (c) **P3** NPs. Bright-field images (d-f). Merged images (g-i). The fluorescence was recorded under 405 nm excitation wavelength. Scar bar: 30 μM.

Conclusions

In summary, we have designed and synthesized a series of AIE-active D-A type conjugated polymers incorporating boron ketoiminate unit as the acceptor. The emission of these polymers can be tuned by introducing monomers with different electron-donating abilities. Furthermore, these polymers nanoparticles can successfully serve as promising fluorescent probes for MCF-7 breast cancer cell imaging due to low cytotoxity and high photosability.

Acknowledgements

This work was supported by the National Natural Science Foundation of China (21174061, 51173078, 21172106, and 21474048) and open project of Beijing National Laboratory for Molecular Sciences.

References

1 (a) E. Wang, Z. Ma, Z. Zhang, P. Henriksson, O. Inganäs, F. Zhang, and M. R. Andersson, *Chem. Commun.*, 2011, **47**, 4908; (b) J. Kim, M. H. Yun, P. Anant, S. Cho, J. Jacob, J. Y. Kim, and C. Yang, *Chem. Eur. J.*, 2011, **17**, 14681; (c) X. Guo, H. Xin, F. S. Kim, A. D. T. Liyanage, S. A. Jenekhe, and M. D. Watson, *Macromolecules*, 2011, **44**, 269; (d) H.-H. Chang, C.-E. Tsai, Y.-Y. Lai, D.-Y. Chiou, S.-L. Hsu, C.-S. Hsu, and Y.-J. Cheng, *Macromolecules*, 2012, **45**, 9282; (e) H.-J. Yun, Y.-J. Lee, S.-J. Yoo, D. S. Chung, Y.-H. Kim, and S.-K. Kwon, *Chem. Eur. J.*, 2013, **19**, 13242; (f) J.-M. Jiang, M.-C. Yuan, K. Dinakaran, A. Hariharan, and K.-H. Wei, *J. Mater. Chem. A*, 2013, **1**, 4415; (g) J. Yuan, Z. Zhai, J. Li, J. Lu, X. Huang, Z. Xu, and W. Ma, *J. Mater. Chem. A*, 2013, **1**, 12128; (h) W. Yue, X. Huang, J. Yuan, W. Ma, F. C. Krebs, and D. Yu, *J. Mater. Chem. A*, 2013, **1**, 10116; (i) P. Dutta, H. Park, W.-H. Lee, I. N. Kang, and S.-H. Lee, *Polym. Chem.*, 2014, **5**, 132; (j) J.-S. Wu, S.-W. Cheng, Y.-J. Cheng and C.-S. Hsu, *Chem. Soc. Rev.*, 2015, **44**, 1113; (k) N. Chakravarthi, K. Gunasekar, C. S. Kim, D.-H. Kim, M. Song, Y. G. Park, J. Y. Lee, Y. Shin, I.-N. Kang, and S.-H. Jin, *Macromolecules*, 2015, **48**, 2454; (l) Z. Xiao, K. Sun, J. Subbiah, T. Qin, S. Lu, B. Purushothaman, D. J. Jones, A. B. Holmesa, and W. W. H. Wong, *Polym. Chem.*, 2015, **6**, 2312.

2 (a) M.-H. Lai, C.-C. Chueh, W.-C. Chen, J.-L. Wu, F.-C. Chen, *J. Polym. Sci., Part A: Polym. Chem.*, 2009, **47**, 973; (b) J. B. Lee, K. H. Kim, C. S. Hong, D. H. Choi, *J. Polym. Sci., Part A: Polym. Chem.*, 2012, **50**, 2809; (c) C. Guo, W. Hong, H. Aziz and Y. Li, *Rev. Adv. Sci. Eng.*, 2012, **1**, 200; (d) Y. Li, P. Sonar, L. Murphy and W. Hong, *Energy Environ. Sci.*, 2013, **6**, 1684; (e) T. W. Lee, D. H. Lee, J. Shin, M. J. Cho, D. H. Choi, *J. Polym. Sci., Part A: Polym. Chem.*, 2013, **51**, 5280; (f) C. Guo, B. Sun, J. Quinn, Z. Yan and Y. Li, *J. Mater. Chem. C*, 2014, **2**, 4289; (g) G. E. Park, J. Shin, D. H. Lee, T. W. Lee, H. Shim, M. J. Cho, S. Pyo, and D. H. Choi, *Macromolecules*, 2014, **47**, 3747.

3 (a) Y. Deng, Y. Chen, X. Zhang, H. Tian, C. Bao, D. Yan, Y. Geng, and F. Wang, *Macromolecules*, 2012, **45**, 8621; (b) B. Balan, C. Vijayakumar, A. Saeki, Y. Koizumi, M. Tsuji and S. Seki, *Polym. Chem.*, 2013, **4**, 2293; (c) J. Wang, X. Chen, Z. Cai, H. Luo, Y. Li, Z. Liu, G. Zhang and D. Zhang, *Polym. Chem.*, 2013, **4**, 5283; (d) X. Zhang, C. Xiao, A. Zhang, F. Yang, H. Dong, Z. Wang, X. Zhan, W. Li and W. Hu, *Polym. Chem.*, 2015, **6**, 4775; (e) M. Jang, J.-H. Kim, D.-H. Hwang, and H. Yang, *ACS Appl. Mater. Interfaces*, 2015, **7**, 12781.

4 S. Ming, S. Zhen, K. Lin, L. Zhao, J. Xu, and B. Lu, *ACS Appl. Mater. Interfaces*, 2015, **7**, 11089.

5 (a) H.-C. Wu, C.-L. Liu and W.-C. Chen, *Polym. Chem.*, 2013, **4**, 5261; (b) Y.-G. Ko, D. M. Kim, K. Kim, S. Jung, D. Wi, T. Michinobu, and M. Ree, *ACS Appl. Mater. Interfaces*, 2014, **6**, 8415; (c) H.-J. Yen, H. Tsai, C.-Y. Kuo, W. Nie, A. D. Mohite, G. Gupta, J. Wang, J.-H. Wu, G.-S. Lioud and H.-L. Wang, *J. Mater. Chem. C*, 2014, **2**, 4374; (d) W. Elsawy, M. Son, J. Jang, M. J. Kim, Y. Ji, T.-W. Kim, H. C. Ko, A. Elbarbary, M.-H. Ham, and J.-S. Lee, *ACS Macro Lett.*, 2015, **4**, 322.

6 M. Helgesen and F. C. Krebs, *Macromolecules*, 2010, **43**, 1253.

7 (a) X. Ma, X. Mao, S. Zhang, X. Huang, Y. Cheng, and C. Zhu, *Polym. Chem.*, 2013, **4**, 520; (b) X. Ma, X. Jiang, S. Zhang, X. Huang, Y. Cheng, and C. Zhu, *Polym. Chem.*, 2013, **4**, 4396.

8 Y. Li, T. Liu, H. Liu, M.-Z. Tian, and Y. Li, *Acc. Chem. Res.*, 2014, **47**, 1186.

9 Y. Hong, J. W. Y. Lamab and B. Z. Tang, *Chem. Soc. Rev.*, 2011, **40**, 5361.

10 (a) D. Ding, K. LI, B. Liu, and B. Z. Tang, *Acc. Chem. Res.*, 2013, **46**, 2441; (b) X. Zhang, X. Zhang, L. Tao, Z. Chi, J. Xu and Yen Wei, *J. Mater. Chem. B*, 2014, **2**, 4398.

11 (a) R. Hu, E. Lager, A. Aguilar-Aguilar, J. Liu, J. W. Y. Lam, H. H. Y. Sung, I. D. Williams, Y. Zhong, K. S. Wong, E. Peña-Cabrera, and B. Z. Tang, *J. Phys. Chem. C*, 2009, **113**, 15845; (b) G.-F. Zhang, M. P. Aldred, W.-L. Gong, C. Li and M.-Q. Zhu, *Chem.*

Commun., 2012, **48**, 7711; (c) W. Z. Yuan, Y. Gong, S. Chen, X. Y. Shen, J. W. Y. Lam, P. Lu, Y. Lu, Z. Wang, R. Hu, N. Xie, H. S. Kwok, Y. Zhang, J. Z. Sun, and B. Z. Tang, *Chem. Mater.*, 2012, **24**, 1518; (d) X. Y. Shen, W. Z. Yuan, Y. Liu, Q. Zhao, P. Lu, Y. Ma, I. D. Williams, A. Qin, J. Z. Sun, and B. Z. Tang, *J. Phys. Chem. C*, 2012, **116**, 10541; (e) Y. Jin and Y. Qian, *New J. Chem.*, 2015, **39**, 2872; (f) T. Jadhav, B. Dhokale, S. M. Mobin and R. Misra, *RSC Adv.*, 2015, **5**, 29878.

12 H. Li, Y. Guo, G. Li, H. Xiao, Y. Lei, X. Huang, J. Chen, H. Wu, J. Ding, and Y. Cheng, *J. Phys. Chem. C*, 2015, **119**, 6737.

13 (a) F. P. Macedo, C. Gwengo, S. V. Lindeman, M. D. Smith and J. R. Gardinier, *Eur. J. Inorg. Chem.*, 2008, 3200; (b) R. Yoshii, A. Nagai, K. Tanaka and Y. Chujo, *Chem. – Eur. J.*, 2013, **19**, 4506; (c) C. Dai, D. Yang, X. Fu, Q. Chen, C. Zhu, Y. Cheng and L. Wang, *Polym. Chem.*, 2015, **6**, 5070.

14 H. Li, Y. Guo, G. Li, H. Xiao, Y. Lei, X. Huang, J. Chen, H. Wu, J. Ding, Y. Cheng, *J. Phys. Chem. C*, 2015, **119**, 6737.

15 (a) Y. Hong, J. W. Y. Lam, B. Z. Tang, *Chem. Commun.*, 2009, 4332; (b) J. Xu, L. Wen, W. Zhou, J. Lv, Y. Guo, M. Zhu, H. Liu, Y. Li, L. Jiang, *J. Phys. Chem. C*, 2009, **113**, 5924; (c) Z. Zhang, B. Xu, J. Su, L. Shen, Y. Xie, H. Tian, *Angew. Chem. Int. Ed.*, 2011, **50**, 11654; (d) X. Shen, Y. Wang, E. Zhao, W. Yuan, Y. Liu, P. Lu, A. Qin, Y. Ma, J. Z. Sun, B. Z. Tang, *J. Phys. Chem. C*, 2013, **117**, 7334; (e) J. Zhang, B. Xu, J. Chen, L. Wang, W. Tian, *J. Phys. Chem. C*, 2013, **117**, 23117; (f) G. Liu, D. Chen, L. Kong, J. Shi, B. Tong, J. Zhi, X. Feng, Y. Dong, *Chem. Commun.*, 2015, **51**, 8555.

16 B. Bao, N. Tao, D. Yang, L. Yuwen, L. Weng, Q. Fan, W. Huang and L. Wang, *Chem. Commun.*, 2013, **49**, 10623.

17 C.-C. Ho, Y.-C. Liu, S.-H. Lin, W.-F Su, *Macromolecules*, 2012, **45**, 813.

18 M. J. Frisch, G. W. Trucks, H. B. Schlegel, G. E. Scuseria, M. A. Robb, J. R. Cheeseman, G. Scalmani, V. Barone, B. Mennucci, G. A. Petersson, H. Nakatsuji, M. Caricato, X. Li, H. P. Hratchian, A. F. Izmaylov, J. Bloino, G. Zheng, J. L. Sonnenberg, M. Hada, M. Ehara, K. Toyota, R. Fukuda, J. Hasegawa, M. Ishida, T. Nakajima, Y. Honda, O. Kitao, H. Nakai, T. Vreven, J. A. Montgomery, Jr, J. E. Peralta, F. Ogliaro, M. Bearpark, J. J. Heyd, E. Brothers, K. N. Kudin, V. N. Staroverov, R. Kobayashi, J. Normand, K. Raghavachari, A. Rendell, J. C. Burant, S. S. Iyengar, J. Tomasi, M. Cossi, N. Rega, J. M. Millam, M. Klene, J. E. Knox, J. B. Cross, V. Bakken, C. Adamo, J. Jaramillo, R. Gomperts, R. E. Stratmann, O. Yazyev, A. J. Austin, R. Cammi, C. Pomelli, J. W. Ochterski, R. L. Martin, K. Morokuma, V. G. Zakrzewski, G. A. Voth, P. Salvador, J. J. Dannenberg, S. Dapprich, A. D. Daniels, Ö. Farkas, J. B. Foresman, J. V. Ortiz, J. Cioslowski and D. J. Fox, Gaussian 09, Revision A.2, Gaussian, Inc., Wallingford CT, 2009.

Graphical abstract

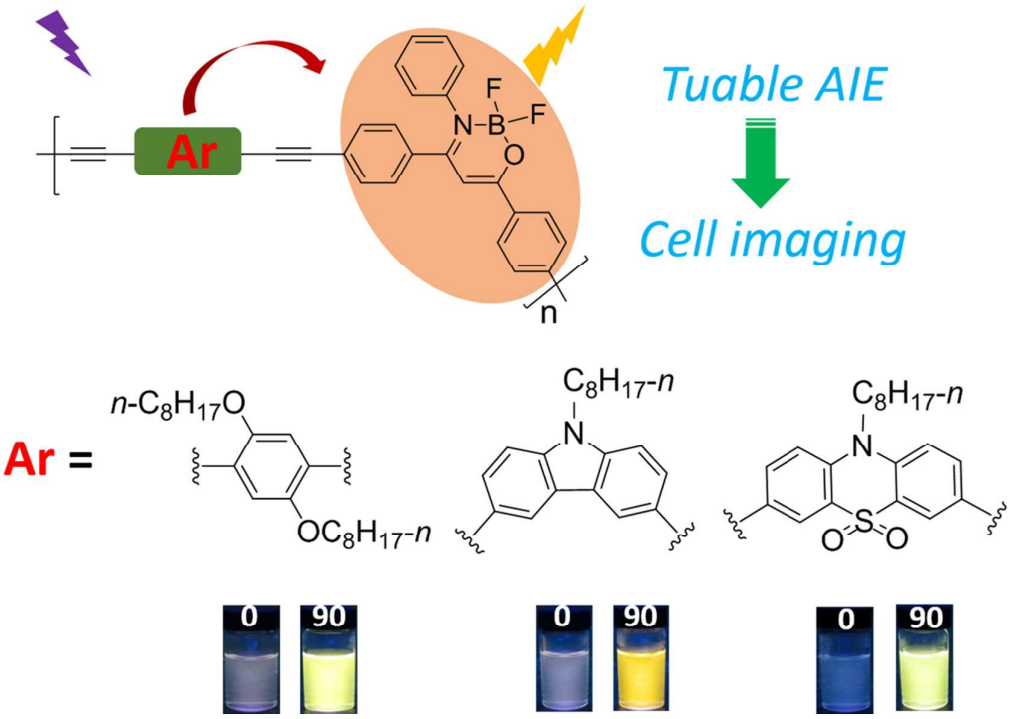

A series of AIE-active D-A type conjugated polymers incorporating boron ketoiminate unit were synthesized and applied for cell imaging.